

## Pore network evaluation of the hydrophysical properties of carbonate rocks (coquinas)

<sup>1</sup>Maira C.O.L. Santo, <sup>2</sup>Mateus. G. Ramirez, <sup>1</sup>Elizabeth M. Pontedeiro, <sup>3</sup>Martinus Th. van Genuchten, <sup>1</sup>José L.D. Alves, <sup>1</sup>Paulo Couto.

<sup>1</sup>*Civil Engineering Department (PEC/COPPE), Federal University of Rio de Janeiro  
Av. Horacio Macedo, bl.B, Centro de Tecnologia, 21945-970, Rio de Janeiro, RJ, Brazil,  
[maira.lima@petroleo.ufrj.br](mailto:maira.lima@petroleo.ufrj.br), [bettymay@petroleo.ufrj.br](mailto:bettymay@petroleo.ufrj.br), [jalves@lamce.coppe.ufrj.br](mailto:jalves@lamce.coppe.ufrj.br), [pcouto@petroleo.ufrj.br](mailto:pcouto@petroleo.ufrj.br)*

<sup>2</sup>*Mechanical Engineering Department (PEM/COPPE), Federal University of Rio de Janeiro  
Av. Horacio Macedo, bl.G, Centro de Tecnologia, 21945-970, Rio de Janeiro, RJ, Brazil  
[mateusgr@poli.ufrj.br](mailto:mateusgr@poli.ufrj.br)*

<sup>3</sup>*Department of Earth Sciences, Utrecht University  
Princetonlaan 8a, Utrecht 3584CB, Netherlands  
[rvangenuchten@hotmail.com](mailto:rvangenuchten@hotmail.com)*

**Abstract.** Carbonate rocks often show nontrivial flow behavior because of their multimodal pore structure. The pore size distribution and pore space topology, the latter describing also how pores are interconnected, can provide much information about the hydraulic behavior of these rocks. Pore Network Modeling (PNM) is an effective method for evaluating petrophysical parameters, including especially the permeability. Pore networks can be generated directly from microCT images to obtain such information as the pore-size distribution, the pore body and pore throat radii distributions, and relevant coordination numbers. The purpose of this paper is to combine microCT, nuclear magnetic resonance (NMR) and mercury intrusion (MICP) techniques to obtain information about petrophysical properties that are not easily measured directly. We were especially interested in comparing microCT, NMR and MICP results, assessing the multi-porosity nature of the coquinas, correlating the permeability with porosity, and obtaining capillary pressure–fluid saturation (Pc-S) relationships. Results were to provide important information about the generally highly heterogeneous nature of carbonate rocks, with as ultimate goal to improve petroleum recovery from oil-bearing carbonate reservoirs. For our study we used four coquina samples from the Morro do Chaves Formation, considered a close analogue of Brazilian Pre-Salt facies. The samples were subjected to routine core analysis, NMR, MICP and microCT scans. The samples had very similar porosities (between 10 and 16%), but different absolute permeabilities (between 5 and 245 mD). Results indicated good correlations, especially between the NMR and microCT data. We further used the mercury intrusion results to obtain estimates of the Pc–S curves. As an example, sample 136.85 showed excellent cross-correlation between the NMR and MICP data, and a well-defined curve of the MICP-derived Pc–S functions for air-water. Plots of the mercury intrusion data and the fitted van Genuchten hydraulic functions indicated a double porosity pore structure.

**Keywords:** Carbonate Rocks, MicroCT, NMR, MICP, Pose-scale Network Modeling

## 1 Introduction

Carbonate rocks contain over 50% of the estimated world oil reserves. Unfortunately, the relationships between porosity and petrophysical properties, traditionally used for reservoir characterizations and oil recovery strategies, are in generally very complex for carbonate rocks [1]. Since they often show nontrivial flow behavior because of their multimodal pore structure, detailed information about their pore size distribution and pore space topology, together with how pores are interconnected, can provide much insight about the hydraulic behavior of carbonate rocks.

In terms of the oil production process, petrophysics is the science that studies the physical, electrical, and mechanical properties of rocks and fluids [2], with a primary aim being to increase oil recovery. Within this

context, the petrophysics of carbonate rocks has received much attention since the discovery of the pre-salt oil-bearing reservoirs in Brazil by Petrobras in 2007. The pre-salt is composed of the Campos and Santos basins, with the reservoirs consisting of three main types of rocks: limestones with coquinas, microbialites in the upper portion of the rift, which were produced and accumulated in lakes connected to the oceans, and fractured volcanic rocks in the lower portion of the rift [3, 4, 5].

For our study we used coquinas as close analogues to those existing in the pre-salt oil reservoirs, aiming to increase knowledge of carbonate rocks. Coquinas are known to be hybrid carbonate rocks; they are formed not exclusively by shells and/or fragments, but also contain significant amounts of siliciclastic material [6]. Such rocks typically have a complex pore system, with pores ranging from micropores to larger vugs, thus making it difficult to accurately estimate specific petrophysical properties such as permeability.

One of the difficulties in predicting the flow behavior in porous media is the high degree of uncertainty associated with determining the quantities that govern fluid retention and flow. The study of pore-scale processes is essential for understanding fluid flow and contaminant transport processes at the continuum or macro scale, which implies a multi-scale problem [7]. These various scales have an associated hierarchy, covering the molecular scale, the micro or pore scale, the macro or laboratory scale, the meso or field scale, and also the mega or regional scale [8].

Pores tend to have irregular forms and surfaces, with many of them sometimes appearing in the form of dead-end pores. These factors influence flow and transport behavior significantly. Pore Network Modeling (PNM) is an effective technique for evaluating petrophysical parameters, including especially the permeability. Networks can be generated directly from x-ray microtomography (microCT) images to obtain such information in a simple and compatible way [9]. The approach typically involves images acquired using microtomography, from which 3D skeletons can be generated. This is done by creating a virtual representation of the porous medium consisting of pore bodies and pore throats of different sizes (the “geometry” of the porous medium) and connected to each other as required (the “topology”), leading to the skeleton of the medium [10]. It is then possible to simulate fluid flow and solute transport processes of interest at the pore scale through this network, with the relevant physics implemented on a pore-to-pore basis, thus providing details of porous media flow and retention parameters that are of fundamental importance for simulating multiphase flow [11].

The goal of this paper is to use microCT, nuclear magnetic resonance (NMR) and mercury intrusion (MICP) to obtain information about petrophysical properties that are not easily measured directly. Our main interest was comparing microCT, NMR and MICP results, assessing the multi-porosity nature of the coquinas, correlating the permeability with porosity, and obtaining information about the capillary pressure–fluid saturation (Pc-S) relationships. Results were to provide important information about the generally highly heterogeneous nature of carbonate rocks, with as ultimate goal to improve petroleum recovery from oil-bearing carbonate reservoirs.

## **2 Materials and Methods**

### **2.1 Coquinas Samples**

For our studies we used 4 coquina samples taken from a continuous test core (UFRJ 2-SMC-02-AL), drilled at Atol Quarry, located in the city of São Miguel dos Campos in the Brazilian state of Alagoas (WGS-8409 ° 45'17"S / 36° 09'14"W), which is part of the Sergipe-Alagoas Basin. The core was provided by the Laboratory of Sedimentary Geology (LAGESED) of UFRJ. All samples had a cylindrical shape, about 2.5 cm in diameter x 4.5 cm in height (Fig.1).

### **2.2 Routine Core Analysis**

The samples were initially subjected to thorough cleaning and the extraction of fluids previously present in the pore system, an essential step for complete removal of impurities contained in the samples. For this stage, Soxhlet extractors were employed using solvents such as toluene for removing hydrocarbons, and methanol for the extraction of salts. This technique ensures complete removal of natural contaminants in a continuous and unsupervised manner, without causing damage to the samples. After cleaning, the samples were dried in an oven at a controlled temperature of 60°C for 12 hours.



Figure 1. Pictures of the coquinas used in this work.

### 2.3 Nuclear Magnetic Resonance (NMR)

The NMR experiments were carried out using a low-field GeoSpac2 spectrometer (Oxford Instruments, UK), having a magnetic field equal to 0.047 T and a frequency of 2 MHz, belonging to the NMR and Petrophysics Applications Laboratory (UFFLAR). All acquisition controls were implemented using GIT software (Green Imaging Technologies, Fredericton, Canada). For the analysis, the samples were saturated with a 30,000 ppm solution of KCl. The analyses were carried out using transversal relaxation measures ( $T_2$ ) obtained by using CPMG pulse sequences, which are commonly used in petrophysical studies [12,13]. A CPMG pulse sequence consists of a  $90^\circ$  radio frequency pulse followed by a pulse train of  $180^\circ$ , delayed by  $\pi/2$  of the first pulse. Echo intensity measurements were performed with a signal/noise ratio above 100.

### 2.4 Mercury Injection Capillary Pressure (MICP)

The MICP experiments were performed using an Autopore IV 9500 (Micromeritics Instruments Co.) Since MICP is a destructive technique, the subsamples for these tests were taken from areas adjacent to the plugs used for the other laboratory experiments. Based on the assumption that fluid is not able to enter the pore opening of a rock pore network without pressure, and that the fluid does not “wet” the pore surface, the MICP tests consist of the gradual injection of mercury using increasing pressures, leading to estimate the ratio of the capillary pressure of the pores and the volume of injected fluid [14]. The experiments begin by enclosing the previously unsaturated sample in a closed container under vacuum, which is then filled with mercury. Starting with atmospheric pressure itself, increasing pressures are subsequently applied to push mercury into the sample. The non-wetting mercury will first invade the larger pores but, with increasing pressures, slowly moves into the entire pore system. Assuming that the pores can be approximated as equivalent cylinders, it is possible to relate the capillary pressure to the radii of pore throats using the Washburn equation [15].

### 2.5 X-Ray Microtomography (MicroCT)

MicroCT imaging techniques allow investigations of the pore structure at scales ranging from micrometers up to a few millimeters. They use the ability of radiation to penetrate materials in varying degrees. The equipment uses a fan-shaped beam geometry to acquire images, which are transmitted by X-ray beams originating from the source, passing through the sample, and being captured by a detector. During acquisition, the sample rotates  $360^\circ$  with steps of  $0.5^\circ$ . At each step, a transmitted image is acquired and saved in 16-bit files (TIFF extensions). After acquisition, the images are reconstructed using specific software from the manufacturer. For the acquisition we used a CoreTOM (Tescan/XRE), belonging to the Advanced Oil Recovery Laboratory (LRAP) of UFRJ, to obtain the images with a  $14 \mu\text{m}$  voxel size, while the images were reconstructed using the Aquila reconstruction software

(Tescan/XRE). Image processing was carried out using Avizo 9.5 (Thermo Fisher Scientific), while the pore network modeling subsequently was carried out using the PoreStudio software, an update of the PoreFlow model of Raouf et al. [9].

### 3 Results

Table 1 shows results of the routine core analyses, such as of porosity and permeability, as well as the PNM modeling, and the NMR results for porosity. As can be seen, the samples had routine porosity values ranging from 10.6% to 16% and permeabilities from 0.98 to 245 mD. The NMR porosity showed a good correlation with the routine porosity measurements, which suggest that the results were satisfactory and the samples were well saturated. Considering routine core analysis as a calibration technique [16], porosity and permeability results from PoreStudio showed lower values with the measurements. This was expected since the microCT resolution did not allow visualization of the entire pore space of the samples but only for pore radii above 7  $\mu\text{m}$ , however allowed to determine the flux at the resolution used.

Table 1. Porosity ( $\Phi$ ) and permeability (K) results obtained using routine core analyses, NMR and PoreStudio modeling

Samples	$\Phi_{\text{rout}}$	$K_{\text{rout}}$	$\Phi_{\text{NMR}}$	$\Phi_{\text{PoreStudio}}$	$K_{\text{PoreStudio}}$
128.05	12.1 %	22.1 mD	13.6 %	4.2 %	18.5 mD
136.85	16 %	245 mD	15 %	12.4 %	202.4 mD
141	11.8 %	4.3 mD	11.1 %	5.5 %	1.64 mD
151.15	10.6%	0.98 mD	10 %	7 %	0.11 mD

Since  $T_2$  distribution reflect the pore size distribution of a rock sample [17], our results clearly indicated that the samples had bimodal and even trimodal distributions. For this study we used the pore size partitioning classification of Silva et al. [18], which describes the heterogeneity of carbonate rock pores. The variations in pore sized within the sample database reinforced the idea of partitioning the pore sizes into five classes: pores with  $T_2$  values up to 1 ms would be considered micropores; between 1 and 10 ms is considered to be a transition region between micro- and mesopores; values between 10 and 100 ms correspond to mesopores; between 100 and 1000 ms is a new transition zone between meso- and macropores; and, finally, the region above 1000 ms is dominated by macropores. Based on this information, Fig. 2a presents the pore distributions for the samples. We noticed that samples 151.15 and 141, which had lower permeabilities, showed  $T_2$  distribution peaks in the macropores region with very similar distributions (bimodal distributions) demonstrating their petrophysical similarity. Samples 128.05 and 136.85 showed a trimodal distribution, with a  $T_2$  distribution peak in different regions, meso/macro hybrid region and macro region, respectively.

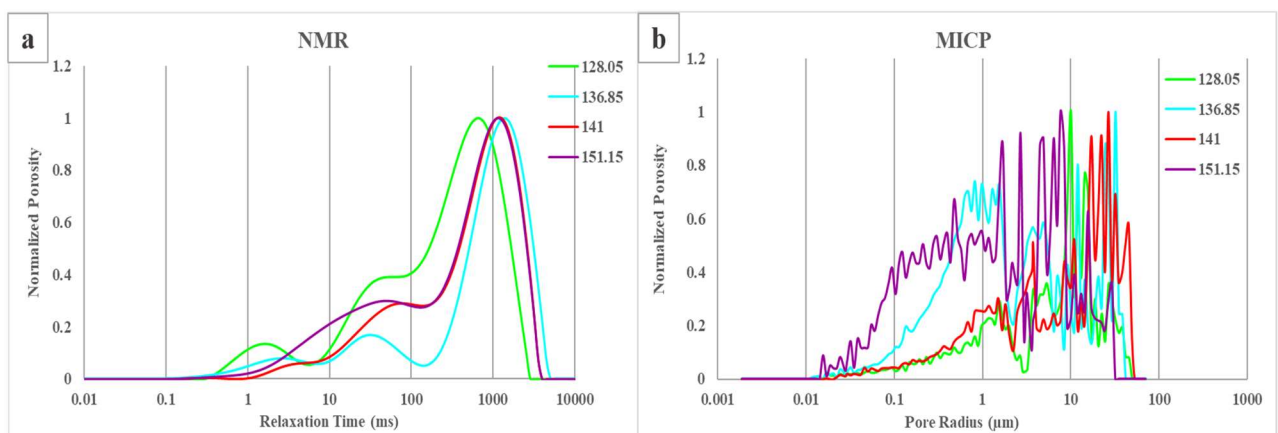


Figure 2. a) NMR graphs of the samples; b) Pore radii distributions of the MICP measurements.

To better understand the permeabilities at the samples, we further conducted MICP measurements. A useful analysis complementary to NMR is the characterization of the distribution of pore apertures (e.g., their radii) using MICP. With this approach the entire pore system, represented by pore bodies (corresponding to the largest voids) and pore throats (connections between the pore bodies) can be evaluated [19]. The distribution of pore throats from the MICP measurements (provided in Fig. 2b), demonstrated that sample 151.15 had throats with the smallest radius, which agrees with its lowest permeability. Regarding sample 136.85, the MICP results shows larger pore throats than sample 151.15 had to higher permeability. Sample 141 showed larger pore radii, but more information is needed in order to understand why that sample had a lower permeability. By injecting mercury stepwise at incremental pressures into a rock medium, MICP techniques can be used to obtain curves of the capillary pressure as a function of mercury saturation. The amount of mercury intrusion at different pressures to which the samples are submitted, shows how difficult is to access the various pores. Initially the larger and more peripheral pores are filled with mercury, after which increasingly smaller pores and more internal (intra-aggregate) pores of the sample will be intruded. The resulting capillary pressure ( $P_c$ ) – saturation ( $S$ ) curves can be compared to assess differences in the pore systems of the samples. Figure 3 shows the  $P_c$ - $S$  curves of the four samples. The curves show an increase in capillary pressure consistent with the entry of mercury into pores having smaller diameters. As can be seen, the pressure is higher for sample 151.15, which is expected to have the lowest permeability of the group. Sample 141, even with a relatively low permeability, had throat aperture similar to sample 128.05. Even sample 136.85, which had the highest permeability and an abundance of macropores (Fig.2a), showed a  $P_c$ - $S$  curve with a marked contribution of micropores to flow. Analysis of the capillary pressure graphs of the samples indicated that 20% of the pores were accessed at similar pressures (below 30 psi). From then on, the pressures of samples 136.85 and 151.15 increased, even though their permeabilities were quite different. To understand these differences, microCT images were used to analyze their porous systems.

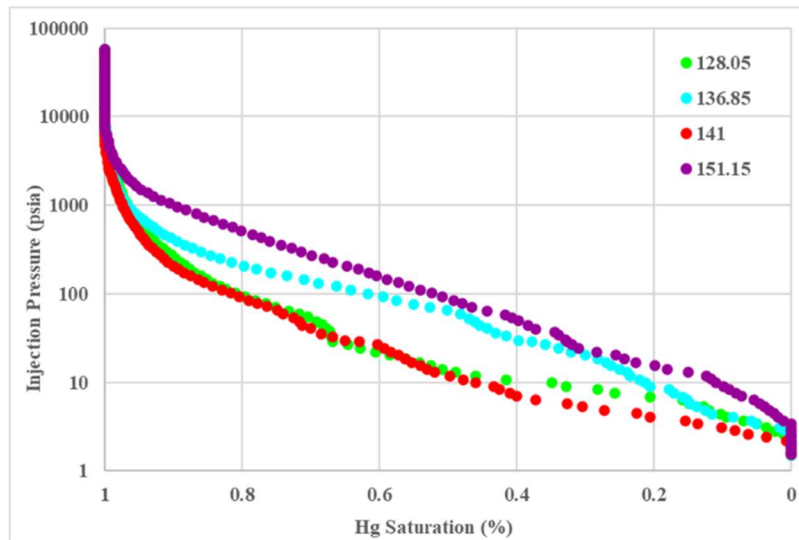


Figure 3. MICP generated capillary pressure curves as a function of mercury saturation for the four samples. Notice the differences in pressure when mercury intrudes the pores at similar saturations.

As mentioned at Lima et al. [13], an important application of the NMR and MICP techniques is integration of the results to determine the surface relaxivity, an essential parameter for calibrating the  $T_2$  curves in order to obtain the pore size distributions. Considering the pore system of the rock as a bundle of cylindrical capillary tubes of radius  $r$ , the distribution of pore throats determined by MICP can be correlated with the distribution of  $T_2$  by means of the surface relaxivity ( $\rho_2$ ), according to:

$$\left(\frac{S}{V}\right)_{cylinder} = \frac{2\pi r l}{\pi r^2 l} = \frac{2}{r} \rightarrow r_{cylinder} = 2\rho_2 T_2 \quad (1)$$

where  $l$  is the length of the capillary. The value 2 in the Eq. (1) is a pore shape parameter to convert the surface to volume ratio ( $S/V$ ) to pore throat radii, which can be changed to 3 for spherical pores. Thus, once a correlation



between the NMR and MICP curves is obtained,  $\rho_2$  can be adjusted until the two curves are consistent [20].

Combining the NMR and MICP measurements will not yield good results if no correlation exists between the pore size distribution curves and the corresponding pore throats. Once visually verified that both distributions (i.e., of mercury saturation and  $T_2$ ) correlated well, we adjusted  $\rho_2$  in Eq. (1) until the distributions had the same maximum, as can be seen in Fig. 4. Samples 136.85 and 151.15 showed some differences between the two curves, notably for MICP radii between 0.1 and 7  $\mu\text{m}$  (sample 136.85) and between 0.1 and 4  $\mu\text{m}$  (sample 151.15), with the NMR curves showing lesser amounts of small pores in those ranges. These results are typical of the situation when the larger pores are surrounded by smaller pores. In this case, the mercury intrudes first the smaller pores that are more external, and subsequently will invade the bigger pores (often referred to as the bottleneck effect). When the acquisition data are processed, the pore volume intruded by mercury is actually measured at a given pressure, and the assumption is that all pores intruded at that volume have the same size. In this way, the larger pores end up being transformed into countless smaller pores with the same diameter, thus increasing their percentage. This effect may explain the significant increase in pores in the micro and micro/meso regions (samples 151.15 and 136.85, respectively), shown by the MICP curves.

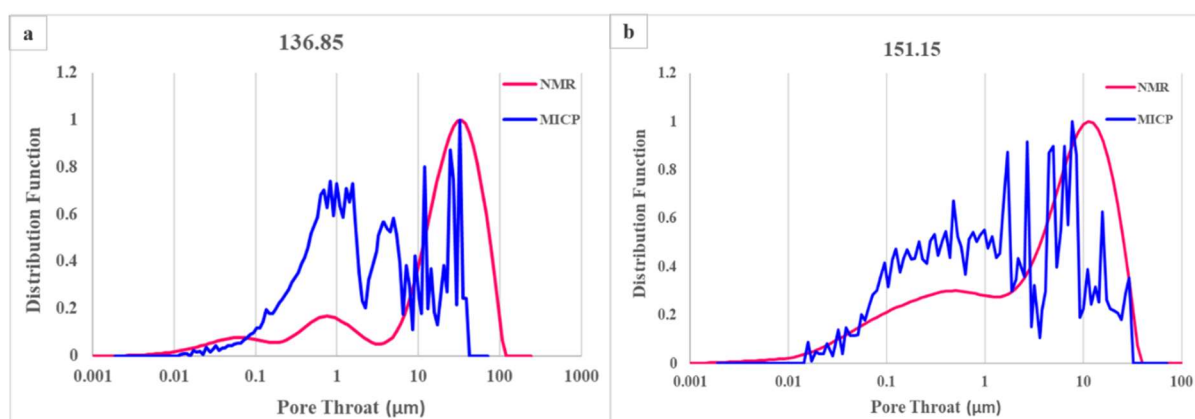


Figure 4. MICP and fitted NMR curves for a) sample 136.85 and b) sample 151.15

Using the Paraview software [21], the pore systems of the samples were visualized to identify the pore bodies and throats that are most connected in the pore system. This will quantify the connected pore groups, in addition to allowing visualization of the main pore clusters connecting to the base and top of the samples. The resulting percolation route should be responsible for most of the flow within the system. The different makeup of the two main percolating clusters in Fig. 5 reflects the different volume of connected pores of the two samples, and their impact on the permeability. In Fig 5a we can visualize the connected pore clusters of sample 136.85, showing different colors for each connected group, with a total of 975 recognized pore groups being quantified. We noticed that the main cluster of this sample, identified with a light blue color, had the most clearly connected pore network within the sample. Since pore network modeling produced a very similar value of the permeability as the routine petrophysical experiments (Table 1), one may conclude that this cluster is responsible for the conductivity of fluid within the pore system. Figure 5b, on the other hand, showed a much broader set of pore clusters for sample 151.15. This sample contained 1923 distinct groups, visibly separated from each other by different colors. It was not possible to identify a main cluster since the pores responsible to connect the various clusters of the sample were below the microCT imaging resolution.

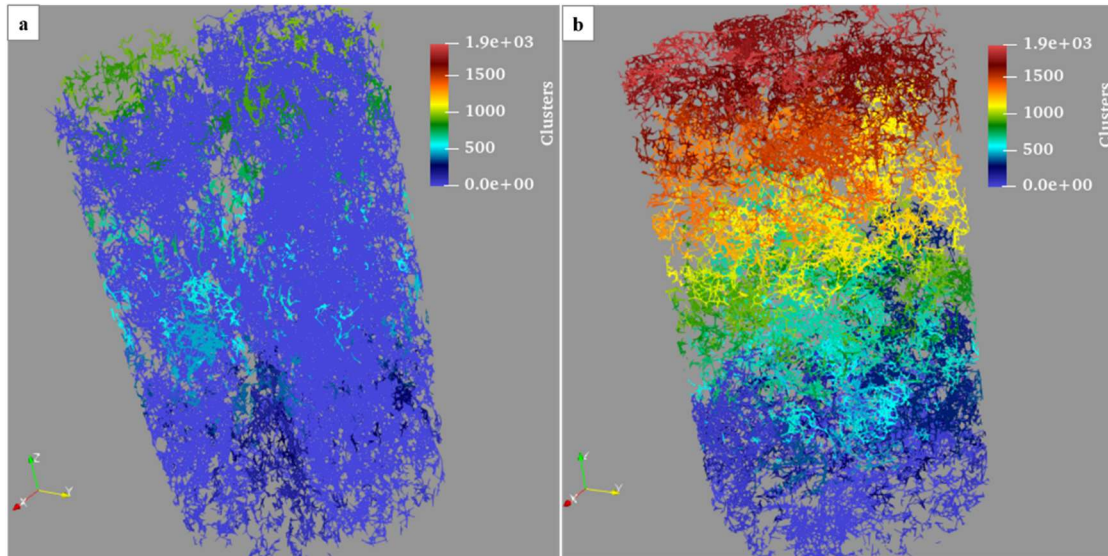


Figure 5. Pore systems of rock sample 136.85 (a) showing its main cluster in light blue, and sample 151.15 (b) showing a much broader set of clusters.

The combined use of NMR and MICP techniques together with microCT imaging and PNM modeling was found to be a very powerful way of analyzing the pore structure of the rock samples, leading to a better understanding of possible fluid flow processes within the pore system. It is important to correlate these data with the continuum through the application of upscaling techniques. In our case we used MICP and NMR data to obtain Pc-S curves. The Pc-S data sets were used as input in a program that provided the van Genuchten hydraulic parameters [22] by using inverse technique. Figure 6 shows the optimized MICP and NMR based dual porosity Pc-S curves. The MICP curve for sample 136.85 showed a tendency for a slightly better fit assuming a triple instead of a dual porosity curve, but more research needs to be conducted in this matter.

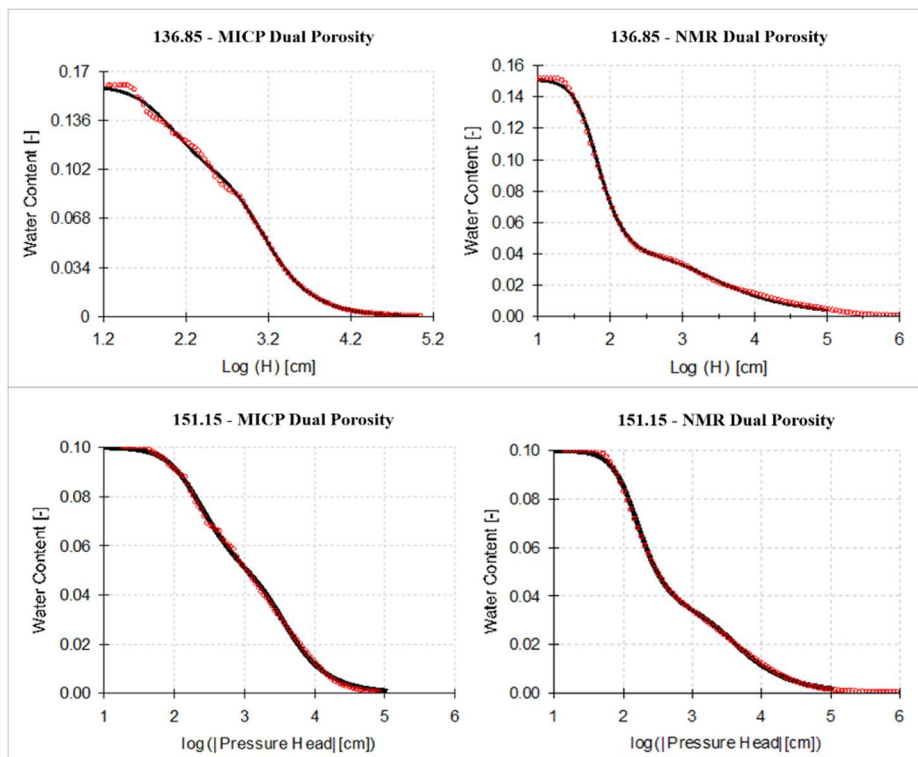


Figure 6. Optimized MICP and NMR based dual porosity Pc-S curves. Data are provided in terms of fluid contents as a function of the pressure head (H) in cm.

## 4 Conclusions

A major focus of this study was to compare microCT, NMR and MICP techniques, thereby assessing the multi-porosity nature of the coquinas, correlating the permeability with porosity, and to obtain information about the capillary pressure – fluid saturation ( $P_c - S$ ) relationships. For this, the effects of pore structure, pore size distribution and capillary pressure were analyzed using four carbonate rock samples having significant permeability variations but similar porosity values. Routine core analyses, NMR and MICP studies were performed on coquina samples from the Morro do Chaves Formation, which is considered a close analogue of Brazilian pre-salt oil reservoirs. Integration of the various methods produced estimates of the surface relaxivity needed to transform relaxation times into the pore size distribution. Threshold values of the distributions, based on the percentage of visible pores at a given resolution, were used (maximum porosity visible in the resolution), considering the pore radius distribution. The microCT images were used to obtain the skeleton, which in turn provided necessary input data (points, segments, and nodes) for porosity and permeability calculations using the PoreStudio pore network modeling software.

**Acknowledgements.** This research was carried out in association with the ongoing R&D projects registered as ANP 19027-2, “Desenvolvimento de infraestrutura para pesquisa e desenvolvimento em recuperação avançada de óleo – EOR no Brasil” (UFRJ/Shell Brasil/ ANP) setting-up a advanced EOR Lab facility for R&D in Brasil, and ANP 20163-2, “Análise experimental da recuperação de petróleo para as rochas carbonáticas do pré-sal brasileiro através da injeção alternada de CO<sub>2</sub> e água”, with samples provided by Project SACL (Análise geológica sedimentar de sucessões carbonáticas do Cretáceo em uma bacia sedimentar brasileira (ANP n.18993-6), all sponsored by Shell Brasil under the ANP R&D levy as “Compromisso de Investimentos com Pesquisa e Desenvolvimento”. This study was financed in part by the Coordenação de Aperfeiçoamento de Pessoal de Nível Superior- Brasil (CAPES) - Finance Code 001, and carried out with the support of CNPq, National Council of Scientific and Technological Development - Brazil. We acknowledge Professor Rodrigo Bagueira (UFF-LAR) for his help saturating the samples and using the NMR equipment. We also thank the research teams of LRAP/COPPE/UFRJ and LAGESED/UFRJ.

**Authorship statement.** The authors hereby confirm that they are the sole liable persons responsible for the authorship of this work, and that all material that has been herein included as part of the present paper is either the property (and authorship) of the authors, or has the permission of the owners to be included here.

## References

- [1] D. Bauer, S. Youssef, M. Fleury, “Improving the estimations of petrophysical transport behavior of carbonate rocks using a dual pore network approach combined with computed microtomography. *Transport in Porous Media*, vol 94, 505–524, 2012. <https://doi.org/10.1007/s11242-012-9941-z>
- [2] D. Tiab, E. Donaldson, “Petrophysics: theory and practice of measuring reservoir rock and fluid transport properties”. *Gulf Professional Publishing*, 2015.
- [3] C. Riccomini, L.G. Sant’Anna, C.C.G. Tassinari, C.C.G. Pré-sal: Geologia e exploração. *Revista USP*, vol. 95, pp. 33-42. 2012 <https://doi.org/10.11606/issn.2316-9036.v0i95p33-42>.
- [4] R.R. Estrella, “Variação da porosidade e da permeabilidade em coquinas da formação Morro do Chaves (Andar Jiquiá), Bacia Sergipe-Alagoas”. *Tcc in Geology* – Universidade Federal do Rio de Janeiro. 2015
- [5] S. Dorobek, L. Piccoli, B. Coffey, A. Adams. “Carbonate rock-forming processes in the pre-salt “sag” successions of Campos Basin, Offshore Brazil: Evidence for seasonal, dominantly abiotic carbonate precipitation, substrate controls, and broader geologic implications”. In: *AAPG Hedberg Conference “Microbial Carbonate Reservoir Characterization”*, 2012.
- [6] A.C Tavares, L. Borghi, P. Corbett, J. Nobre-Lopes, R. Câmara, “Facies and depositional environments for the coquinas of the Morro do Chaves Formation, Sergipe-Alagoas Basin, defined by taphonomic and compositional criteria”. *Brazilian Journal of Geology* 2015. <http://dx.doi.org/10.1590/2317-488920150030211>
- [7] X. Yang, H. Sun, H., Y. Yang, Y. Liu, X. Li, X., “Recent progress in multi-scale modeling and simulation of flow and solute transport in porous media”. *Wiley Interdisciplinary Reviews: Water*, vol. 8, 2021. <https://doi.org/10.1002/wat2.1561>
- [8] M.C.O.L. Santo, “The effects of the pore connectivity on the permeability of coquinas (carbonate rocks) from the Morro do Chaves Formation, Sergipe-Alagoas basin, Brazil”. PhD thesis, Universidade Federal do Rio de Janeiro, 2020.
- [9] A. Raouf, H.M. Nick, S.M. Hassanizadeh, C.J. Spiers, “PoreFlow: A complex pore-network model for simulation of reactive transport in variably saturated porous media”. *Computers & Geosciences*, vol 61, pp. 160-174, 2013.



- [10] D. Wildenschild, A.P. Sheppard, “X-ray imaging and analysis techniques for quantifying pore-scale structure and processes in subsurface porous medium systems”. *Advances in Water Resources*, vol. 51, pp. 217-246. 2013. <https://doi.org/10.1016/j.advwatres.2012.07.018>
- [11] T. Silveira, F. Hoerlle, A. Rocha, M.C.O. Lima, M.G. Ramirez, E.M. Pontedeiro, M.Th. van Genuchten, D. Cruz, P. Couto, “Effects of carbonated water injection on the pore system of a carbonate rock (coquina)”. *Journal of Hydrology and Hydromechanics*, vol. 70. 2022. <https://doi.org/10.2478/johh-2022-0001>.
- [12] M. Fleury, M. Romero-Sarmiento, “Characterization of shales using  $T_1$ - $T_2$  NMR maps”. *Journal of Petroleum Science and Engineering*, vol. 137, pp. 55-62. 2016. <https://doi.org/10.1016/j.petrol.2015.11.006>
- [13] M.C.O. Lima, E.M. Pontedeiro, M.G. Ramirez, A. Boyd, M.Th. van Genuchten, L. Borghi, P. Couto, A. Raouf, “Petrophysical correlations for permeability of coquinas (carbonate rocks)”. *Transport in Porous Media*, vol. 135, pp. 287-308. 2020 <https://doi.org/10.1007/s11242-020-01474-1>
- [14] J. Shafer, J. Neasham, “Mercury porosimetry protocol for rapid determination of petrophysical and reservoir quality properties”. *International Symposium of the Society of Core Analysts*. Society for Core Analysts Fredericton, Canada, 2000.
- [15] E.W. Washburn, “The dynamics of capillary flow”. *Physics Reviews* 1921. <https://doi.org/10.1103/PhysRev.17.273>
- [16] C. McPhee, J. Reed, I. Zubizarreta. Core sample preparation. In: *Core analysis: A best Practice Guide*, pp. 138-143. Elsevier. 2015.
- [17] E.H. Rios, I. Figueiredo, A. Muhammed, R.B.V. Azeredo, A. Moss, T. Pritchard, B. Glassborow. NMR permeability estimators under different relaxation time selections: a laboratory study of cretaceous diagenetic chalks, SPWLA, 55<sup>th</sup> Annual Logging Symposium. 2014.
- [18] P.N., Silva, E.C., Gonçalves, E.H., Rios, A., Muhammad, A. Moss, T. Pritchard, B. Glassborow, A., Plastino, R.B.V. Azeredo. Automatic classification of carbonate rocks permeability from <sup>1</sup>H NMR relaxation data. *Expert Systems with Applications*. 2015. <https://doi.org/10.1016/j.eswa.2015.01.034>
- [19] Y. Yuan, R. Rezaee. Comparative Porosity and Pore Structure Assessment in Shales: Measurement Techniques, Influencing Factors and Implications for Reservoir Characterization. *Energies*, vol.12, pp.2094. 2019 <https://doi.org/10.3390/en12112094>
- [20] A.A. Souza, G. Carneiro, L. Zielinski, R. Polinski, L. Schwartz, M.D. Hurlimann, A. Boyd, E.H. Rios, W.A. Trevizan, B.C.C. Santos, V.F. Machado, R.B.V. Azeredo. Permeability prediction improvement using 2D Difusion-T2 Maps. SPWLA, 54<sup>th</sup> Annual Logging Symposium. 2013
- [21] U. Ayachit. The ParaView Guide: A Parallel Visualization Application. Kitware. 2015.
- [22] E. Priesack, W. Durner, “Closed-form expression for the multi-modal unsaturated conductivity function”. *Vadose Zone Journal*, vol. 5, n. 1, pp. 121–124, 2006. <https://doi.org/10.2136/vzj2005.0066>